Magnetic Ordering and Frustration in Hexagonal UNi_4B

S. A. M. Mentink,[1] A. Drost,[2] G. J. Nieuwenhuys,[1] E. Frikkee,[2] A. A. Menovsky,[1] and J. A. Mydosh[1]
[1]*Kamerlingh Onnes Laboratory, Leiden University, P.O. Box 9506, 2300 RA Leiden, The Netherlands*
[2]*Netherlands Energy Research Foundation ECN, P.O. Box 1, 1755 ZG Petten, The Netherlands*
(Received 3 May 1994)

We have determined unusual magnetic ordering of the hexagonal intermetallic uranium compound UNi_4B via neutron diffraction. In the easy basal plane the U moments have triangular symmetry with antiferromagnetic interactions. Along the hard c axis ferromagnetic coupling occurs. Below $T_N = 20$ K only two out of every three U moments of $1.2\mu_B$ order in vortexlike arrangements around the third paramagnetic spin. This novel magnetic structure is related to the occurrence of a crystallographic superstructure. Previously observed anomalies in bulk properties below T_N are attributed to unconventional spin-wave excitations associated with this type of ordering.

PACS numbers: 75.20.Hr, 75.25.+z, 75.30.Gw

Hexagonal intermetallic compounds with $CaCu_5$-type crystal structures compose a variety of interesting ground states, among which are the newly discovered antiferromagnetic (AF) heavy-fermion superconductors UNi_2Al_3 [1,2] and UPd_2Al_3 [3–5] and permanent magnet materials like $SmCo_4B$ [6]. Furthermore, and seemingly unrelated, there has been much recent interest in (insulating) magnetic materials with antiferromagnetic coupling, often on triangular lattices, where ordering at temperatures corresponding to the exchange energies is prevented by geometric frustration [7,8]. In such cases, unusual magnetic order and critical phenomena are found.

These two subjects coalesce with the metallic triangular, uranium compound UNi_4B [9,10]. Here basal-plane AF interactions between U moments (Ni is nonmagnetic) lead to a unique type of magnetic ordering, with Néel temperature $T_N = 20$ K. The zero-field magnetic structure of UNi_4B can be described by a magnetic unit cell of nine U atoms. However, only six of these atoms order below T_N in an AF hexagonal pattern in the basal plane, with ferromagnetic (FM) coupling along c; the other three U atoms remain paramagnetic. The paramagnetic nature of the U moments on every third lattice site causes highly anomalous magnetic and transport behavior in the ordered state. In this Letter we introduce the basic properties of UNi_4B, describe our single-crystal neutron-diffraction results, and illustrate the magnetic structure. We discuss its implications for bulk properties and evaluate the nature of the low-energy magnetic excitations.

The structure of UNi_4B is related to the hexagonal $CeCo_4B$-type crystal structure, space-group $P6/mmm$, with lattice parameters $a = 4.953$ Å and $c = 6.964$ Å [9]. The experiments presented here are performed on Czochralski-grown single crystals of high quality as evaluated by electron probe microanalysis and neutron diffraction. We used the ^{11}B isotope for the crystal investigated by neutron diffraction. The crystals were not given additional heat treatment. Sample-dependent properties were not observed in our series of polycrystalline and single-crystalline specimens, some of which were annealed at 700 °C for one week [11]. In contrast to earlier conclusions drawn from powder x-ray diffraction, the more accurate single-crystal neutron-diffraction experiments reveal the occurrence of a crystallographic superstructure, which is quite common in RNi_4B (R = rare earth) materials [12]. We have not found any indications of a structural transition below 365 K. As shown below, the superstructure is important for understanding the bulk magnetic properties of UNi_4B, which are displayed in Fig. 1.

The susceptibility (defined by the magnetization divided by the applied field), measured in a superconducting quantum interference device magnetometer in 0.3 mT and 0.5 T, is strongly anisotropic, with an easy (hexagonal) a-b plane; see Fig. 1(a). Above 100 K, the effective U moment equals $2.90\mu_B$/f.u. with f.u. representing formula units, with Curie-Weiss parameter $\Theta_{CW} = -65$ K. The ordering temperature $T_N = 20$ K is defined by the maximum in $\partial(\chi T)/\partial T$. Below T_N, χ_{ab} increases, which is not expected for a normal antiferromagnet, before a saturation takes place below around 10 K. At larger fields a maximum occurs, without signs of field-history effects. Figure 1(b) shows the low-temperature part of the electrical resistivity, $\rho(T)$, measured by a standard dc four-lead technique down to 380 mK. The resistivity parallel to the basal plane, $\rho_{\parallel a}$, is 3 times larger than along the c axis, $\rho_{\parallel c}$. This large anisotropy is even more pronounced in the ordered state, where the initial increase in $\rho_{\parallel a}$ indicates the formation of new superzone boundaries due to the AF ordering. In contrast, $\rho_{\parallel c}$ exhibits an immediate drop at T_N, indicative of FM ordering along the c direction. For both directions, a reduction of the scattering is observed below $T = 5$ K. Below T_N, $\rho_{\parallel c}$ is accurately described by

$$\rho_{\parallel c} = AT^{0.11} + BT^2 \qquad (1)$$

with coefficients $A = 57.995(1)\ \mu\Omega\,\mathrm{cm/K^{0.11}}$ and $B = 3.79977(6) \times 10^{-2}\ \mu\Omega\,\mathrm{cm/K^2}$. Finally, the specific heat, $c(T)$, of UNi_4B also displays unusual behavior in the ordered state. Figure 1(c) depicts $c(T)/T$ down to 1.8 K. A sharp anomaly signals the long-range AF order below

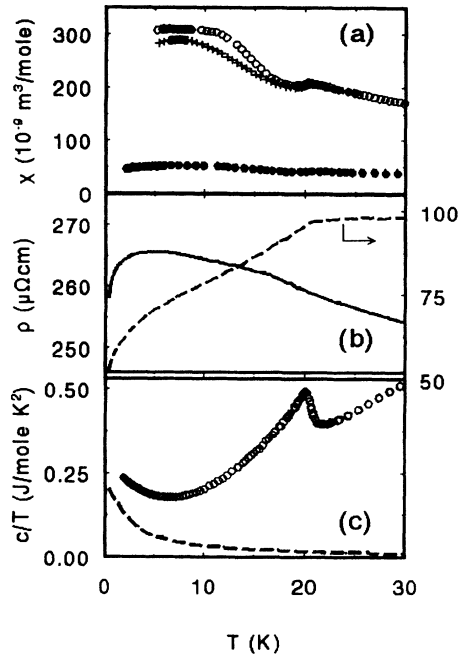

FIG. 1. Magnetic properties of single-crystalline UNi_4B below 30 K. (a) Susceptibility, $\chi \equiv M/H$, with the magnetic field parallel to the easy a-b plane: (○) $\mu_0 H = 0.3$ mT, (+) $\mu_0 H = 0.5$ T; and the hard c axis: (•)$\mu_0 H = 0.5$ T. (b) Zero-field resistivity with current along to the a-b plane (—) and the c axis (– – –). Note the different absolute scales and the unconventional temperature dependences in the ordered state. (c) Zero-field specific heat divided by temperature, showing an increase below 7 K. The dashed line represents the calculated specific heat for a 1D Heisenberg ferromagnetic chain with $S = 1/2$ and $Jc = 35$ K, according to Ref. 13.

20 K. However, after an initial drop, c/T starts increasing again upon lowering the temperature below 7 K. Magnetic fields up to 6 T do not significantly influence the low-temperature specific heat [9]. After subtraction of the phonon-derived specific heat of nonmagnetic UCo_2Ni_2B, the magnetic entropy recovered at 25 K amounts to $0.72R$ ln2 [10,11]. Analogous to $\rho(T)$, the magnetic specific heat in the ordered state is best described by a weak power-law dependence:

$$c/T = \alpha T^{-0.29} + \beta T^2 \qquad (2)$$

with coefficients $\alpha = 0.2796(7)$ J/mole $K^{1.71}$ and $\beta = 0.3913(9) \times 10^{-3}$ J/mole K^4. The dashed line in Fig. 1(c) indicates the calculated specific heat divided by T for the 1D Heisenberg ferromagnetic chain with $S = 1/2$ and $Jc/k_B = 35$ K according to Bonner and Fisher [13].

Neutron-diffraction measurements were performed between 2.4 K and 365 K on a $UNi_4{}^{11}B$ single crystal at the triple-axis spectrometer HB3 of the high-flux reactor in Petten, using a wavelength $\lambda = 1.4269$ Å and a pyrolytic graphite filter to suppress higher-order wavelengths in the beam. We studied both the nuclear and magnetic reflections in the (a^*b^*0) and (a^*0c^*) scattering planes. All strong nuclear reflections can be indexed on the basis of a hexagonal subcell with $a_{sub} = 4.953$ Å and $c_{sub} = 6.964$ Å at 293 K [11,14]. However, additional reflections occur with Miller indices $(\frac{h-k}{3}\ \frac{h+2k}{3}\ 0)$, proving the existence of a superstructure. Their intensities are 2 or 3 orders of magnitude weaker than the main reflections. In real space the hexagonal unit cell of the superstructure is related to the subcell by a rotation over 30° in the basal plane with an elongation of a by a factor $\sqrt{3}$, giving supercell lattice parameters $a' = \sqrt{3}a$ and $c' = c$. We also observed $(\frac{h}{6}\ \frac{k}{6}\ l)$ reflections, leading to an even larger nuclear supercell. These reflections are again 1 or more orders of magnitude weaker than the $(\frac{h-k}{3}\ \frac{h+2k}{3}\ 0)$ reflections, and are *not* surrounded by magnetic satellites.

Below $T_N = 21(1)$ K we observe magnetic intensity at distances $\pm\vec{Q} = (\frac{1}{3}\ \frac{1}{3}\ 0)_{\text{super}}$ from the reciprocal lattice points of the superstructure, as shown in Fig. 2. This $\vec{Q}$ vector describes the magnetic order, leading to a hexagonal magnetic unit cell with axes parallel to those of the subcell, and $a_{\text{magn}} = 3a_{\text{sub}}$. The absence of magnetic $(h\,k\,1)$ and the presence of magnetic $(h\,k\,2)$ reflections give $c_{\text{magn}} = \frac{1}{2}c_{\text{sub}}$. From the observed intensities we derived the ordered magnetic pattern, displayed in Fig. 3. The measured and calculated intensities, giving a reliability factor $R = 11.2\%$, are listed in Table I. We find that six U moments are ordered in two triangular sublattices of next-nearest neighbors, with moments perpendicular to the c axis and 120° apart, while the directions for the remaining three moments *are not defined*. The symmetry of the surrounding moments suggests a paramagnetic behavior for these three moments. This also follows directly from the diffraction data. An ordering of the three moments, uncorrelated with the other six moments, would give a scaled contribution of 7 to I_{calc} for the $(\frac{2}{3}\ \frac{1}{3}\ 0)$ reflection, in contradiction to the very weak intensity observed. In addition, an ordering of the three moments, correlated with the other six moments, would yield large differences between the $(\frac{1}{3}\ 0\ 0)$, $(0\ \frac{1}{3}\ 0)$, and $(\frac{1}{3}\ -\frac{1}{3}\ 0)$ in-

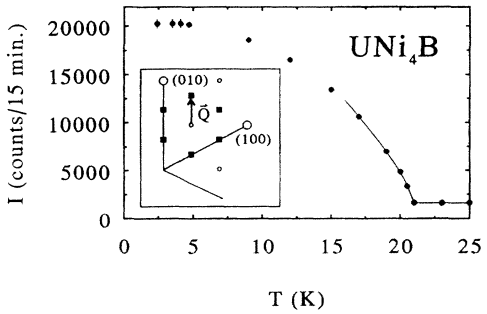

FIG. 2. Temperature dependence of the $(\frac{2}{3}\,0\,0)$ maximum intensity; the solid line is a fit by Eq. (3) for 5 data points below $T_N = 21(1)$ K, indicating a critical exponent $\beta = 0.38(2)$. The ordered magnetic moment amounts to $1.2\mu_B$/U. No additional anomalies are observed below T_N. The inset shows the weak supercell reflections (○) and magnetic reflections (■) in the reciprocal lattice of the substructure (○). The magnetic ordering vector $\vec{Q} = (\frac{1}{3}\ \frac{1}{3}\ 0)_{\text{super}}$ corresponds to $(0\ \frac{1}{3}\ 0)_{\text{sub}}$.

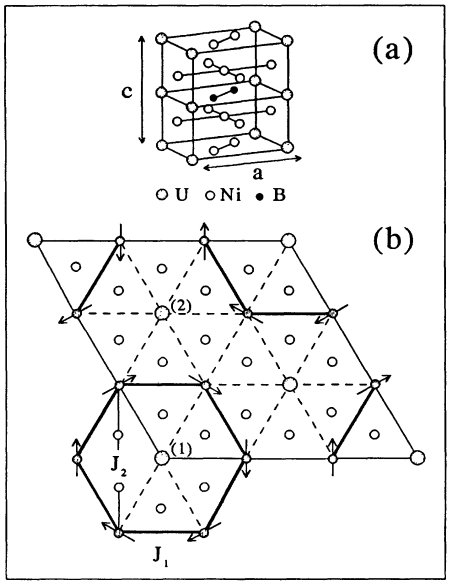

FIG. 3. (a) Crystallographic $CeCo_4B$-type *subcell* of UNi_4B. (b) Magnetic structure of hexagonal UNi_4B, projected onto the basal plane. The magnetic layers are stacked ferromagnetically along the c direction. The thin solid lines represent the magnetic unit cell. Note the presence of the frustrated U spins, indicated by (1) and (2), with two inequivalent magnetic environments, located in the center of the magnetic vortices (thick lines). The nearest and next-nearest neighbor magnetic coupling constants are indicated by J_1 and J_2.

tensities, which are not observed. We can distinguish two paramagnetic sites: the (0 0 0) site, (1) in Fig. 3(b), which is surrounded by a tangential vortex formed by six 60° spin rotations, and the $(\frac{1}{3}\,\frac{2}{3}\,0)$ and $(\frac{2}{3}\,\frac{1}{3}\,0)$ sites, (2) in Fig. 3(b), surrounded by three AF pairs. Note that the magnetic structure factors F_{magn} depend on the moment direction in the proposed magnetic structure. For example, a rotation of all six ordered moments over 30° would result in $F_{\mathrm{magn}} = 0$ for the $(\frac{1}{3}\,0\,0)$ reflection. We have computer generated a few hundred magnetic structures within the same magnetic unit cell. None of these simulated structures were in agreement with the experimental results of the neutron diffraction. There were always some of the magnetic reflections incorrectly absent or present.

A rough analysis of the critical behavior of the $(\frac{2}{3}\,0\,0)$ reflection intensity I by

$$I = A\epsilon^{2\beta} + B, \quad \epsilon \equiv \frac{T_N - T}{T_N} \tag{3}$$

shows that the magnetic order in UNi_4B follows the prediction for the three-dimensional XY model with a critical exponent $\beta = 0.38(2)$ (solid line in Fig. 2). From the saturation value at 4 K of the integrated magnetic intensities of the $(\frac{2}{3}\,0\,0)$ and $(\frac{1}{3}\,0\,2)$ reflections and the reported U form factor [15] we estimate the ordered moment $\mu_{\mathrm{ord}} = 1.2(2)\mu_B$/(U atom). This value agrees with the local fields, as measured in our recent muon spin rotation experiments [16]. Between 4 K and 2.4 K

TABLE I. Scaled integrated magnetic intensities of single-crystal $UNi_4{}^{11}B$ at 4 K compared with the calculated intensity $I_{\mathrm{calc}} = |F_{\mathrm{magn}}/p|^2/\sin 2\theta$ with $p = 0.2696 \times 10^{-14}$ m. The Miller indices are chosen with respect to the subcell. The reliability factor $R = 100\sum|(I_{\mathrm{obs}} - I_{\mathrm{calc}})|/\sum I_{\mathrm{obs}}$ equals 11.2%.

$h\,k\,l$	I_{obs}	I_{calc}	$h\,k\,l$	I_{obs}	I_{calc}
$(\frac{1}{6}\,0\,0)$	0	0	$(\frac{1}{3}\,0\,1)$	0	0
$(\frac{1}{3}\,0\,0)$	75.3	79.4	$(\frac{2}{3}\,0\,1)$	0	0
$(\frac{2}{3}\,0\,0)$	37.3	36.4	$(\frac{1}{3}\,0\,2)$	20.5	21.8
$(\frac{1}{3}\,\frac{1}{3}\,0)$	0	0	$(\frac{2}{3}\,0\,2)$	12.7	18.1
$(\frac{2}{3}\,\frac{1}{3}\,0)$	1.0	1.0	$(\frac{4}{3}\,0\,2)$	16.0	10.5
$(\frac{4}{3}\,0\,0)$	17.6	15.5	$(\frac{5}{3}\,0\,2)$	9.7	7.7
$(\frac{5}{3}\,0\,0)$	9.7	10.7			

the intensities of the strongest magnetic reflections did not change. A more detailed account of the neutron-diffraction experiments will be published elsewhere [14].

Figure 3 displays both the $CeCo_4B$-type subcell and the magnetic structure, projected onto the basal plane. Every U layer exhibits similar moment directions, for the interactions along the c axis are FM. The derived vortexlike magnetic structure of UNi_4B is to our knowledge unique in hexagonal systems. Since the magnetic interactions in the basal plane are AF, the triangular symmetry implies topological frustration, counteracting long-range magnetic order [8]. This should result in strong frustration of the magentic ordering and modified critical behavior. However, we propose that the formation of the crystallographic superstructure partially lifts this frustration by a change in the site symmetry of the U ions. We assume that the U atoms nearly ideally occupy their (subcell) 1(a) and 1(b) positions and that the nickel and boron atoms are slightly displaced out of their ideal subcell equilibrium positions. The relatively strong $(\frac{h}{3}\,0\,1)$ and weak $(\frac{h}{3}\,0\,2)$ structural reflections [11,14] indicate that atoms in planes separated by a distance $c/2$ are displaced in antiphase with each other. Electronically, this superstructure provides a small periodic change in the crystal-field potential at the U site, which modifies the triangular symmetry. Determination of the exact nature of the superstructure is a subject for future study [14].

The occurrence of paramagnetic moments in an ordered matrix is very rare. We have found no additional ordering phenomena down to 0.38 K in these single crystals, and down to 40 mK by resistivity measurements on a polycrystalline sample. We can now analyze the consequences of this unique combination of magnetic order and paramagnetism for the low-temperature anomalies presented in Fig. 1. The peak in the susceptibility and specific heat at 20 K reflects the ordering of the six U spins. Both the in-field and zero-field experiments indicate that the remaining three U atoms carry

entropy, and thus are also magnetic, with moment direction in the a-b plane. Because of the small U interatomic distance along the c axis, the direct U-5f electron hybridization is rather strong [10]. In combination with the FM coupling along c, this results in the formation of short-range correlated paramagnetic chains in the c direction. These paramagnetic moments within the ordered system form a unique realization of 1D ferromagnetic chain in a metal. Upon lowering the temperature, the specific heat of these chains indeed follows the "normal" behavior of a 1D ferromagnet, e.g., $CsNiF_2$, [17] as calculated by Bonner and Fisher [13]; see dashed line in Fig. 1(c). A similar comparison for the magnetic susceptibility is more difficult to make due to the diverging susceptibility expected for a ferromagnetic chain [17]. However, we do not wish to stress the analogy between the above insulator and our metallic and partially ordered UNi_4B. Note that spins *a priori* cannot order in one dimension. Since the molecular fields arising from the ordered spins cancel at every site of a free spin, as confirmed in our recent muon spin rotation experiments [16], these spins do not undergo a cooperative phase transition. With decreasing T, the increasing correlation length along the chains causes the saturation of the susceptibility and subsequent decrease for larger fields [13]. Also, the extra magnetic scattering evident in the low-temperature resistivity can now be understood. The excitations in the chains of short-range correlated moments are effective scatterers of conductions electrons moving perpendicular to the chains. Only when these excitations freeze out, $\rho(T)$ drops rapidly. Also rather large negative magnetoresistances are found [11]. The upturn in c/T, which corresponds to a broad maximum in the specific heat, indicates a slow removal of entropy. The unusual temperature dependence fitted by Eq. (2) involves a T^2 term due to regular AF spin waves, arising from the ordered spins, and a term $\propto T^{-0.29}$, which stems from the magnetic excitations of the ferromagnetically coupled chains. In our high-field magnetization experiments several spin-flop transitions have been observed, depending on the in-plane field direction [9]. Even in 50 T the magnetization still does not saturate. This implies AF in-plane nearest and next-nearest neighbor couplings, indicated by J_1 and J_2 in Fig. 3. The role of the paramagnetic spins in the high-field magnetization process is still unknown and may only be determined experimentally by neutron diffraction. Note that all J_1-energy terms cancel, and the sum of J_2 terms equals $-3|J_2|$ (but cancel at the paramagnetic sites). This is the lowest energy possible, and all next-nearest spins indeed align at 120° angles in each sublattice of three moments.

Because the paramagnetic moments, making up 1/3 of the spins, are coupled by a J_2 interaction among themselves, it is remarkable that these moments do not develop long-range magnetic order. Such could be either correlated or uncorrelated with the other 2/3 of the spins which order at 20 K. This should be contrasted with the Ising and triangular system $CsCoBr_3$, where 2/3 of the spins order at 28 K and the remaining 1/3 order at 12 K [18]. Hence, we must conjecture that different site symmetries of the U ions in the observed crystalline superstructure alter the interaction J_2 in such a way as to inhibit magnetic order for the surviving 1/3 moments. Certainly this point warrants further investigation.

In conclusion, we have discovered a novel magnetic ordering pattern in the hexagonal metallic compound UNi_4B, whose magnetic unit cell of nine spins contains three paramagnetic spins. This separation into two magnetic subsystems gives rise to anomalous behavior in the ordered state. The simple metallurgy and (subcell) crystal structure of UNi_4B presents the unique opportunity to experimentally and theoretically study magnetic interactions, excitations, and critical behavior of a material which adopts an unprecedented ordered magnetic structure, incorporating chains of paramagnetic spins, on a hexagonal lattice in a metal.

Part of this research was supported by the Stichting voor Fundamenteel Onderzoek der Materie (FOM), which is financially supported by the Nederlandse Organisatie voor Wetenschappelijk Onderzoek (NWO).

[1] C. Geibel *et al.*, Z. Phys B **83**, 305 (1991).
[2] A. Schröder *et al.*, Phys. Rev. Lett. **72**, 136 (1994).
[3] C. Geibel *et al.*, Z. Phys. B **84**, 1 (1991).
[4] A. Krimmel *et al.*, Solid State Commun. **87**, 829 (1993).
[5] R. Caspary *et al.*, Phys. Rev. Lett. **71**, 2146 (1993).
[6] See, e.g., K.J. Strnat, in *Ferromagnetic Materials Vol.4*, edited by E.P. Wohlfarth and K.H.J. Buschow (Elsevier, Amsterdam, 1988) p. 131.
[7] A.P. Ramirez, Annu. Rev. Mater. Sci. **24**, 453 (1994).
[8] See, e.g., M.L. Plumer *et al.*, in *Magnetic Systems with Competing Interactions*, edited by H.T. Diep, (World Scientific, Singapore, 1994).
[9] S.A.M. Mentink *et al.*, Physica (Amsterdam) **186-188B**, 270 (1993).
[10] S.A.M. Mentink *et al.*, Physica (Amsterdam) **194-196B**, 275 (1994).
[11] S.A.M. Mentink, Ph.D. thesis, Leiden University, 1994, (unpublished).
[12] F.E. Spada *et al.*, Phys. Rev. B **30**, 4909 (1984).
[13] J.C. Bonner and M.E. Fisher, Phys. Rev. A **135**, 640 (1964).
[14] A. Drost *et al.* (to be published).
[15] J.P. Desclaux and A.J. Freeman, in *Handbook on the Physics and Chemistry of the Actinides, Vol.1*, edited by A.J. Freeman and G.L. Lander (North-Holland, Amsterdam, 1984), p. 46.
[16] G.J. Nieuwenhuys *et al.* (to be published).
[17] M. Steiner, J. Villain, and C. Windsor, Adv. Phys. **25**, 87 (1976).
[18] W.B. Yelon, D.E. Cox, and M. Eibschütz, Phys. Rev. B **12**, 5007 (1975); A. Farkas, B.D. Gaulin, Z. Tun, and B. Briat, J. Appl. Phys. **69**, 6167 (1991).

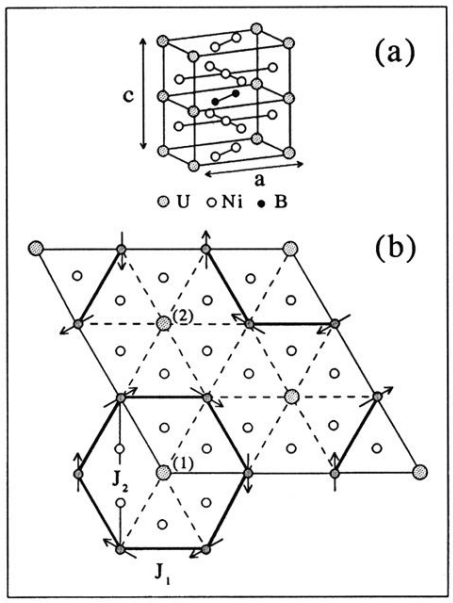

FIG. 3. (a) Crystallographic $CeCo_4B$-type *subcell* of UNi_4B. (b) Magnetic structure of hexagonal UNi_4B, projected onto the basal plane. The magnetic layers are stacked ferromagnetically along the c direction. The thin solid lines represent the magnetic unit cell. Note the presence of the frustrated U spins, indicated by (1) and (2), with two inequivalent magnetic environments, located in the center of the magnetic vortices (thick lines). The nearest and next-nearest neighbor magnetic coupling constants are indicated by J_1 and J_2.